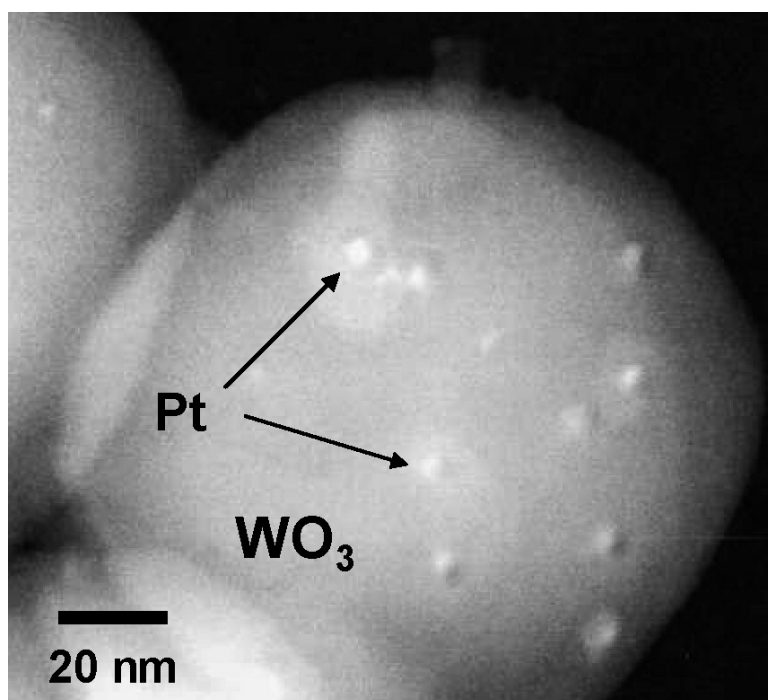


Pristine Simple Oxides as Visible Light Driven Photocatalysts: Highly Efficient Decomposition of Organic Compounds over Platinum-Loaded Tungsten Oxide

Ryu Abe, Hitoshi Takami, Naoya Murakami, and Bunsho Ohtani

J. Am. Chem. Soc., **2008**, 130 (25), 7780-7781 • DOI: 10.1021/ja800835q • Publication Date (Web): 31 May 2008

Downloaded from <http://pubs.acs.org> on February 8, 2009



More About This Article

Additional resources and features associated with this article are available within the HTML version:

- Supporting Information
- Links to the 4 articles that cite this article, as of the time of this article download
- Access to high resolution figures
- Links to articles and content related to this article
- Copyright permission to reproduce figures and/or text from this article

[View the Full Text HTML](#)



Pristine Simple Oxides as Visible Light Driven Photocatalysts: Highly Efficient Decomposition of Organic Compounds over Platinum-Loaded Tungsten Oxide

Ryu Abe,^{*,†,‡} Hitoshi Takami,[‡] Naoya Murakami,[‡] and Bunsho Ohtani^{†,‡}

Catalysis Research Center, Hokkaido University, Sapporo 001-0021, Japan, and Graduate School of Environmental Earth Science, Hokkaido University, Sapporo 060-0810, Japan

Received February 1, 2008; E-mail: ryu-abe@cat.hokudai.ac.jp

The development of visible light driven photocatalysts has been an active research field in recent years,^{1–7} with most research focused on achieving efficient decomposition of environmental organic contaminants under sunlight or indoor fluorescent light. It is generally considered that the conduction band (CB) level of a semiconductor should be more negative than the potential for the single-electron reduction of oxygen ($O_2 + e^- = O_2^-$ (aq), -0.284 V vs NHE; $O_2 + H^+ + e^- = HO_2$ (aq), -0.046 V vs NHE) in order to allow efficient consumption of photoexcited electrons and subsequent oxidative decomposition of organic compounds by holes to proceed in air. Recent studies have focused on the introduction of midgap levels above the top of the O 2p valence band (VB) of titanium oxide (e.g., nitrogen- or sulfur-doped TiO_2),^{1,2} as well as hybridization of the O 2p with other orbitals such as N 2p (e.g., oxynitrides),^{3,5} to achieve both visible light absorption and a sufficiently negative CB level for O_2 reduction. On the other hand, the CB levels of simple oxide semiconductors with visible light absorption, such as tungsten oxide (WO_3), are generally more positive (e.g., $+0.5$ V vs NHE for WO_3) than the reduction potentials of O_2 due to the deeply positive level of VB, which mainly consists of O 2p orbitals.⁸ This fact has so far led us to believe that WO_3 is unsuitable for achieving the efficient oxidative decomposition of organic compounds in air and limited the use of WO_3 photocatalysts to reactions with strong electron acceptors.⁹ Only a few studies have so far been reported on the oxidative decomposition of organic compounds using WO_3 or its composite-type photocatalysts.^{7,10} In the present study, WO_3 loaded with nanoparticulate Pt is demonstrated to exhibit high efficiency for the decomposition of organic compounds under visible light irradiation. Transient photoabsorption analysis by photoacoustic (PA) spectroscopy reveals that the photoexcited electrons in WO_3 are reactive toward O_2 , and that the reaction rate is enhanced considerably by loading with particulate platinum, certainly due to promotion of multielectron O_2 reduction.

Platinum-loaded WO_3 samples (Pt- WO_3) were prepared with a photodeposition method from $H_2PtCl_6 \cdot 6H_2O$ on fine particulate WO_3 (50–200 nm, ca. 10.5 m² g⁻¹) under visible light irradiation in pure water and subsequently in an aqueous methanol (10 vol %) solution. This procedure resulted in a highly uniform dispersion of platinum particles (average size, 5 nm) on the WO_3 surface. The detail procedure and the scanning transmission electron microscopy (STEM) images of the Pt- WO_3 powder are provided in the Supporting Information (Figure S1). A homemade nitrogen-doped TiO_2 (N- TiO_2 , ca. 88.9 m² g⁻¹) was prepared as a reference sample according to the previously reported method.^{1b}

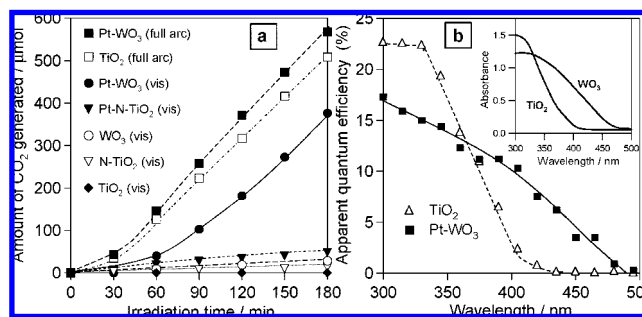


Figure 1. (a) Time course of CO_2 evolution over TiO_2 (P25), Pt- WO_3 (1 wt % Pt), bare WO_3 , Pt-N- TiO_2 (1 wt % Pt), and N- TiO_2 photocatalysts suspended in aqueous acetic acid solution under full-arc ($300 < \lambda < 500$ nm) or visible light irradiation ($400 < \lambda < 500$ nm). (b) Action spectra of acetic acid decomposition over Pt- WO_3 and TiO_2 photocatalysts.

Figure 1a shows the time courses of CO_2 generation over WO_3 , TiO_2 (P25), and N- TiO_2 photocatalysts suspended in aqueous acetic acid solution (AcOH aq). Under full-arc irradiation from a xenon lamp ($\lambda > 300$ nm), the rate of CO_2 generation over Pt- WO_3 photocatalyst (1 wt % Pt) is higher than that over TiO_2 . Whereas CO_2 generation over TiO_2 photocatalyst is negligible under visible light ($\lambda > 400$ nm), Pt- WO_3 exhibits relatively high activity for CO_2 generation, achieving a rate comparable to that under full-arc irradiation. The rate of CO_2 generation over WO_3 from aqueous AcOH increased remarkably with increasing Pt loading to a maximum of $230 \mu\text{mol h}^{-1} CO_2$ at 1 wt % Pt. This rate of CO_2 generation is ca. 30 times higher than that over bare WO_3 ($8 \mu\text{mol h}^{-1}$). Although detectable amounts of CO_2 gas were generated over N- TiO_2 , the rate (ca. $12.0 \mu\text{mol h}^{-1}$ with optimal Pt loading) was much lower than that over Pt- WO_3 . The action spectrum (Figure 1b) for Pt- WO_3 resembles the photoabsorption spectrum of WO_3 , indicating that the decomposition of AcOH can be ascribed to the band gap photoexcitation of WO_3 .

The change in the amount of acetaldehyde (AcH) and CO_2 in the gas phase during reactions over the photocatalysts is shown in Figure 2a. With the onset of visible irradiation, the amount of AcH in the gas phase over Pt- WO_3 (0.1 wt % Pt) decreased rapidly accompanied by an increase in CO_2 generation. The final molar amount of CO_2 (ca. $30 \mu\text{mol}$) is twice that of the AcH injected, indicating that complete decomposition of AcH ($CH_3CHO + 5/2O_2 \rightarrow 2CO_2 + 2H_2O$) proceeds in this reaction. Stable CO_2 generation was observed over N- TiO_2 , although at a rate (ca. $5.3 \mu\text{mol h}^{-1}$) much lower than that over Pt- WO_3 (ca. $70 \mu\text{mol h}^{-1}$), even with optimal Pt loading. In the case of AcH decomposition, appreciable CO_2 generation was observed even over bare WO_3 in the initial period of irradiation. However, CO_2 generation reached saturation within 20 min, before complete decomposition of AcH. This is likely to be attributable to the accumulation of stable intermediates

[†] Catalysis Research Center.

[‡] Graduate School of Environmental Earth Science.

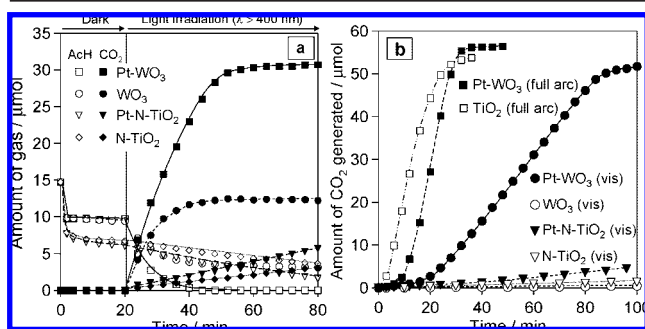


Figure 2. (a) Time course of acetaldehyde (1000 ppm, ca. 15 μmol) decomposition over Pt-WO₃ (0.1 wt % Pt), bare WO₃, Pt-N-TiO₂ (0.5 wt % Pt), and bare N-TiO₂ under visible irradiation (400 < λ < 500 nm). (b) Time course of CO₂ generation from IPA (1200 ppm, ca. 17 μmol) over the photocatalysts under full-arc or visible light irradiation.

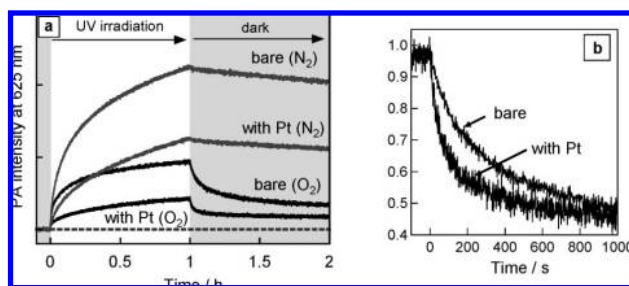


Figure 3. (a) Progression of PA signal at 625 nm during reactions over bare and Pt-WO₃ (0.05 wt % Pt). (b) Normalized decay profiles of PA intensity in the dark.

on the surface of WO₃, as suggested by Sayama et al.⁷ Figure 2b shows the time course of isopropyl alcohol (IPA) decomposition for the photocatalysts. In this case, an optimal Pt loading (0.5 wt %) onto WO₃ photocatalyst resulted in a complete decomposition of IPA with ca. 100-fold enhanced CO₂ generation rate (from 0.4 to 48 $\mu\text{mol h}^{-1}$), while only 4-fold increase was observed for N-TiO₂ by optimal Pt loading. The CO₂ generation rate over Pt-WO₃ was almost comparable to that over TiO₂ when compared under full-arc irradiation ($\lambda > 300$ nm).

These results strongly suggest that the photoexcited electrons in WO₃ are reactive toward O₂, especially when loaded with Pt, contradicting the general understanding that the CB level of WO₃ is insufficient to reduce O₂. The reactivity of photoexcited electrons in WO₃ was analyzed using a double-beam PA spectroscopic technique recently developed by our group.¹¹ The PA spectrum of bare WO₃ under UV irradiation in the presence of air and IPA vapor exhibits an upward shift in the visible region at wavelengths longer than 470 nm (Figure S2). This shift is attributable to the accumulation of pentavalent tungsten (W⁵⁺), which has a broad absorption in the visible region,¹² by the capture of photoexcited electrons at trapping sites in WO₃ (counterpart of hole consumption by IPA). The time course of PA intensity at a fixed wavelength of 625 nm is shown in Figure 3a for bare and Pt-loaded WO₃ samples. Under an N₂ atmosphere, the PA intensity increases rapidly when exposed to UV irradiation and then decreases slowly in the dark. In the presence of O₂, W⁵⁺ accumulation is suppressed, and the PA intensity decreases rapidly when irradiation is ceased. These results indicate that W⁵⁺ is consumed through electron transfer from W⁵⁺ to O₂, regenerating the original hexavalent tungsten (W⁶⁺). Loading with a small amount of Pt (0.05 wt %) enhances the decay of W⁵⁺ considerably in the dark (Figure 3b). The accumulation of W⁵⁺ could not be observed under UV irradiation in the presence of O₂ for WO₃ loaded with more than 0.5 wt % Pt, indicating that the

photoexcited electrons react efficiently with O₂ before being trapped to generate W⁵⁺. It can thus be concluded that the photoexcited electrons in WO₃ are reactive toward O₂, and that the reaction is accelerated considerably by Pt loading. It is known that the potential of multielectron reduction of O₂ is more positive (e.g., O₂ + 2H⁺ + 2e⁻ = H₂O₂ (aq), +0.682 V; O₂ + 4H⁺ + 4e⁻ = 2H₂O, +1.23 V) than for the single-electron process. It seems reasonable to consider that such multielectron reductions more readily proceed on the surface of Pt that works as an electron pool and catalyzes O₂ reduction, compared to the bare surface of oxide semiconductors, while the formation of H₂O₂ over TiO₂ has been reported in the presence of a particular electron donor.¹³ The high activity of Pt-WO₃ is therefore likely to be due to the promotion of multielectron reduction of O₂ on the Pt cocatalyst rather than single-electron reduction, which is generally considered the main pathway for electron consumption over TiO₂ and N-TiO₂ photocatalysts.^{1c,14} This is reasonably supported by the result that the Pt-associated enhancement of the photocatalytic activity of TiO₂ (not shown) and N-TiO₂ was considerably less than that for WO₃ since both photocatalysts possessing sufficient CB level for the reduction of O₂ by single electron.

In summary, WO₃ loaded with nanoparticulate Pt was demonstrated to exhibit high photocatalytic activity for the decomposition of organic compounds both in liquid and gas phases; the activity was almost comparable to that of TiO₂ under UV light irradiation and much higher than that of N-TiO₂ under visible irradiation. The present results indicate that loading with a particulate cocatalyst to promote multielectron O₂ reduction is an effective strategy for the development of highly efficient and durable visible light driven photocatalysts based on simple oxides.

Acknowledgment. This work was supported by a Grant-in-Aid for Scientific Research on Priority Areas (No. 19028004, "Chemistry of Concerto Catalysis") from the Ministry of Education, Culture, Sports, Science and Technology, Japan

Supporting Information Available: Detailed preparation procedure and STEM image of Pt-WO₃, experimental conditions for photocatalytic activity test, and PA spectrum. This material is available free of charge via the Internet at <http://pubs.acs.org>.

References

- (1) (a) Asahi, R.; Morikawa, T.; Ohwaki, T.; Aoki, K.; Taga, Y. *Science* **2001**, *293*, 269–271. (b) Irie, H.; Watanabe, Y.; Hashimoto, K. *J. Phys. Chem. B* **2003**, *107*, 5483–5486. (c) Mrowetz, M.; Balcerski, W.; Colussi, A. J.; Hoffmann, M. R. *J. Phys. Chem. B* **2004**, *108*, 17269–17273.
- (2) Ohno, T.; Mitsui, T.; Matsumura, M. *Chem. Lett.* **2003**, *32*, 364–365.
- (3) Ito, S.; Ravindranathan, K.; Comte, P.; Liska, P.; Grätzel, M. *Chem. Commun.* **2005**, *na*, 268–270.
- (4) Kim, H. G.; Hwang, D. W.; Lee, J. S. *J. Am. Chem. Soc.* **2004**, *126*, 8912–8913.
- (5) Maeda, K.; Takata, T.; Hara, M.; Saito, N.; Inoue, Y.; Kobayashi, H.; Domen, K. *J. Am. Chem. Soc.* **2005**, *127*, 8286–8287.
- (6) Nakamura, R.; Okamoto, A.; Osawa, H.; Irie, H.; Hashimoto, K. *J. Am. Chem. Soc.* **2007**, *129*, 9596–9597.
- (7) Arai, T.; Yanagida, M.; Konishi, Y.; Iwasaki, Y.; Sugihara, H.; Sayama, K. *J. Phys. Chem. C* **2007**, *111*, 7574–7577.
- (8) Scaife, D. E. *Solar Energy* **1980**, *25*, 41–54.
- (9) (a) Darwent, J. R.; Mills, A. *J. Chem. Soc., Faraday Trans. 2* **1982**, *78*, 359–367. (b) Erbs, W.; Desilvestro, J.; Borgarello, E.; Grätzel, M. *J. Phys. Chem.* **1984**, *88*, 4001–4006. (c) Abe, R.; Sayama, K.; Sugihara, H. *J. Phys. Chem. B* **2005**, *109*, 16052–16061.
- (10) Scalfani, A.; Palmisano, L.; Marci, G.; Venezia, A. M. *Sol. Energy Mater. Sol. Cells* **1998**, *51*, 203–219.
- (11) Murakami, N.; Prieto Mahaney, O. P.; Abe, R.; Torimoto, T.; Ohtani, B. *J. Phys. Chem. C* **2007**, *111*, 11927–11935.
- (12) Feish, T. H.; Mains, G. J. *J. Chem. Phys.* **1982**, *76*, 780–786.
- (13) Kormann, C.; Bahnemann, D.; Hofmann, M. R. *Environ. Sci. Technol.* **1988**, *22*, 798–806.
- (14) (a) Ishibashi, K.; Fujishima, A.; Watanabe, T.; Hashimoto, K. *J. Phys. Chem. B* **2000**, *104*, 4933–4938. (b) Hirakawa, T.; Nosaka, Y. *Langmuir* **2002**, *18*, 3247–3254.

JA800835Q